Volodymyr Babizhetskyy*, Volodymyr Levytskyy, Volodymyr Smetana, Magdalena Wilk-Kozubek, Oksana Tsisar, Lyudmyla Piskach, Oleg Parasyuk[a] and Anja-Verena Mudring

New cation-disordered quaternary selenides $Tl_2Ga_2TtSe_6$ (Tt = Ge, Sn)

https://doi.org/10.1515/znb-2019-0169
Received October 24, 2019; accepted November 17, 2019

Abstract: Two new quaternary selenides of the α-TlSe structure type have been synthesized and characterized. Single crystal X-ray diffraction analysis has revealed that $Tl_2Ga_2SnSe_6$ crystallizes with space group *I*4/*mmc*, $a = 8.095(1)$, $c = 6.402(1)$ Å, with a refined composition of $Tl_{1-x}Ga_{1-y}Sn_ySe_2$ ($x = y = 0.345(5)$), $Z = 4$, $R1 = 0.028$; $wR2 = 0.066$. The crystal structure of the isostructural compound $Tl_2Ga_2GeSe_6$ has been determined by means of powder X-ray diffraction: space group *I*4/*mmc*, $Z = 4$, $a = 8.0770(4)$, $c = 6.2572(5)$ Å, refined composition $Tl_{1-x}Ga_{1-y}Ge_ySe_2$, $x = 0.343(5)$, $y = 0.35(2)$, ($R_{B(I)} = 0.084$; $R_P = 0.041$; $R_{Pw} = 0.058$). According to their optical absorption spectra all compounds are semiconductors with relatively narrow direct band gaps of 2.15(3) and 2.05(5) eV for the Ge and Sn phase, respectively.

Keywords: crystal structure; gallium; thallium; tin; selenide.

Dedicated to: Professor Arndt Simon on the occasion of his 80th birthday.

1 Introduction

The family of binary Tl*X* (*X* = S, Se, Te) compounds and their derivatives is well known as optical and semiconducting materials [1]. Ordered ternary representatives $TlTtX_2$ (*Tt* = Al, Ga, In) also exist featuring two crystallographic sites with different coordination environments, but the existence of solid solutions for different chalcogenides cannot be excluded [2–6]. The light atoms in those structures usually exhibit the oxidation state +3, while the heavy ones rather adopt the oxidation state +1. This fact provoked further investigation towards formation of solid solutions or quaternary compounds in the series $TlTtX_2$–$Tt'X_2$ (*Tt'* = Si, Ge, Sn) exhibiting aliovalent metal substitutions.

It should be noted that a few representatives of the $Tt''TtX_2$–$Tt'X_2$ systems are known with *Tt''* = Li, Na, Cu, Ag having approximate stoichiometry $Tt''_2Tt_2Tt'X_6$. For instance, lithium-containing systems with gallium include the $Li_2Ga_2GeS_6$ compound that crystallizes in the non-centrosymmetric orthorhombic space group *Fdd*2 which is a promising non-linear optical material [7]. The substitution of In for Ga results in a series of compounds $Li_2In_2Si(Ge)S_6(Se_6)$ that crystallize in a monoclinic structure, space group *Cc* [8, 9]. Isostructural sodium-containing compounds $Na_2In_2Si(Ge)S_6(Se_6)$ and $Na_2CdGe_2S_6(Se_6)$ have also been reported [10–13]. It has been found that $Na_2Ga_2GeS_6$ crystallizes in the orthorhombic structure (space group *Fdd*2), while $Na_2In_2SiS_6$ and $Na_2In_2GeS_6$ have monoclinic structures (space group *Cc*). $Na_2Ga_2SnS_6$ is dimorphic and crystallizes in both of the above structures.

The formation of the 2-2-1-6 compounds is also common in silver-containing systems. They all crystallize in either of two structures. The monoclinic structure (space group *Cc*) is typical of indium-containing compounds ($Ag_2In_2Si(Ge)S_6$ [14], $Ag_2In_2SiSe_6$ [15], $Ag_2In_2GeSe_6$ [16]), while compounds with Ga ($Ag_2Ga_2SiS_6$ [17], $Ag_2Ga_2SiSe_6$ [18]) crystallize in the tetragonal structure (space group $I\bar{4}2d$). Finally, unique cases of this composition are known in a copper-containing system $Cu_2In_2SiS_6$ (space group *Cc*) [19] and in a combination with thallium, $Tl_2In_2SnSe_6$ (space group *I*4/*mcm*) [20].

[a]Deceased.

***Corresponding author: Volodymyr Babizhetskyy,** Department of Inorganic Chemistry, Ivan Franko National University of Lviv, Kyryla and Mefodiya Street 6, UA-79005 Lviv, Ukraine, e-mail: v.babizhetskyy@googlemail.com
Volodymyr Levytskyy: Department of Inorganic Chemistry, Ivan Franko National University of Lviv, Kyryla and Mefodiya Street 6, UA-79005 Lviv, Ukraine
Volodymyr Smetana and Anja-Verena Mudring: Department of Materials and Environmental Chemistry, Stockholm University, Svante Arrhenius väg 16C, Stockholm 10691, Sweden
Magdalena Wilk-Kozubek: Department of Materials and Environmental Chemistry, Stockholm University, Svante Arrhenius väg 16C, Stockholm 10691, Sweden; and ŁUKASIEWICZ Research Network – PORT Polish Center for Technology Development, 147 Stabłowicka Street, 54-066 Wrocław, Poland
Oksana Tsisar, Lyudmyla Piskach and Oleg Parasyuk: Department of Inorganic and Physical Chemistry, Lesya Ukrainka Eastern European National University, 13 Voli av., 43025 Lutsk, Ukraine

For that reason, the $TlGaSe_2$–$SnSe_2$ system has been investigated in more detail, followed by iso-compositional representatives with Ge. At ambient conditions $TlGaSe_2$ has a monoclinic crystal structure [10] (structure type $KInS_2$ [21]), whereas a tetragonal structure (high-temperature inherent variant, α-TlSe type [6]) has been observed within the $TlGaSe_2$–$SnSe_2$ cross-section. The composition, defined by energy-dispersive X-ray spectroscopy (EDX), indicated the existence of a new quaternary compound. In this work we present the results of structural, spectroscopic and theoretical investigations of the nonstoichiometric $Tl_{1-x}Ga_{1-x}Tt_xSe_2$ series.

2 Experimental

2.1 Synthesis

The $Tl_2Ga_2TtSe_6$ samples were prepared from high-purity elements (Tl, 99.99 wt.%; Ga, 99.999 wt.%; Si, 99.9999 wt.%; Ge, 99.9999 wt.%; Sn, 99.9999 wt.%; Se, 99.999 wt.%). Single crystals of $Tl_2Ga_2TtSe_6$ were grown using the Bridgman-Stockbarger method [22]. Crystals were synthesized and grown in fused silica ampoules with a conical bottom. Calculated amounts of 37 mol% $GeSe_2$/63 mol% $TlGaSe_2$ and 40 mol% $SnSe_2$/60 mol% $TlGaSe_2$ with the total weights of 2 g were placed in a fused silica tube, evacuated to a residual pressure of 0.1 Pa, and then sealed. The samples were synthesized in a shaft-type furnace by heating to T = 1170 K at the rate of 40 K · h^{-1}. The melt was kept at this temperature for 6 h with periodic vibration to assure homogeneity, cooled to T = 870 K at the rate of 20 K · h^{-1}, and annealed for 10 days. The process ended in cooling the ampoule to room temperature at 8.4 K · h^{-1}.

2.2 Microprobe analysis

Quantitative sample analysis was performed by the EDX technique with a scanning electron microscope REMMA-102-02. EDX analysis of pieces of mechanically crushed samples showed that the $Tl_2Ga_2SnSe_6$ sample was homogeneous and its chemical composition corresponded to $Tl_{18.7(2)}Ga_{21.0(3)}Sn_{8.8(2)}Se_{51.5(3)}$. The $Tl_2Ga_2GeSe_6$ sample average is $Tl_{19(1)}Ga_{20(2)}Ge_{10(2)}Se_{51(2)}$ in good agreement with the nominal sample composition, though the refined Se content using this method is slightly underestimated compared to the loaded one.

2.3 X-ray single-crystal diffraction

A shiny metallic black needle-shaped single crystal was isolated from the crushed sample. Its quality was evaluated by the Laue method using white X-ray Mo radiation. The single-crystal X-ray diffraction data were collected at room temperature on a STOE IPDS II image plate diffractometer with monochromatized Mo$K\alpha$ radiation.

The unit cell parameters and extinction rules suggested $I4/mcm$ as the most appropriate space group. The WinGX program package [23] was used for the hkl data treatment. Multi-scan absorption corrections were made with the use of the program Platon [24]. The basic model of the crystal structure was obtained by Direct Methods using the program Sir2014 [25]. Only three different atomic coordinates were obtained (in 4a, 4b and 8h positions) equivalent to those of β-$TlGaSe_2$ [6]. First the Tl, Ga and Se atoms were appointed in 4a, 4b and 8h positions, according to the β-$TlGaSe_2$ structure, respectively. Refinement of the crystal structure with the program Shelxl [26] in isotropic approximation of atomic displacement showed three residual electron density peaks in the difference Fourier synthesis close to the Tl atom (10.7 e Å^{-3}; 0.59 Å) and a high reliability factor $R1$ = 0.163. Anisotropic refinement yielded a substantial decrease of $R1$ to 9.8% but still a considerable (9.1 e Å^{-3}) residual electron density peak at the Ga position. Statistical occupation of the 4b and partial occupation of the 4a positions revealed significant improvement of the R values and a satisfactory chemical composition with respect to the EDX analysis ($R1$ = 0.028; $wR2$ = 0.066; S = 1.154; $Tl_{0.655}Ga_{0.657}Sn_{0.343}Se_2$). Finally, taking into account the valences of the elements, the refinement was simplified for a more reasonable form $Tl_{1-x}Ga_{1-y}Sn_xSe_2$, $x = y = 0.345(5)$. The refined composition is close to the initial value $Tl_2Ga_2SnSe_6$, indicating a narrow homogeneity range of the compound. The crystal data and information on data collection and evaluation are summarized in Table 1. The atomic coordinates, equivalent and anisotropic displacement parameters and interatomic distances are listed in Tables 2–4, respectively. Crystal structure illustrations have been prepared with the program Diamond [27].

2.4 X-ray powder diffraction

Experimental diffraction data for the isostructural compounds $Tl_2Ga_2GeSe_6$ and $Tl_2Ga_2GeSe_6$ were obtained on a DRON 4-13 diffractometer (45 kV and 30 mA, Cu$K\alpha$ radiation, Bragg-Brentano geometry) and analyzed with the WinCSD program package [28].

Table 1: Crystal data and structure refinement details of $Tl_2Ga_2SnSe_6$.

Empirical formula	$Tl_2Ga_2SnSe_6$
Moiety formula	$Tl_{1-x}Ga_{1-y}Sn_ySe_2$, $x=y=0.345(5)$
Equal to composition (in at.%)	$Tl_{17.9}Ga_{17.9}Sn_{9.5}Se_{54.7}$
Composition by EDX (in at.%)	$Tl_{18.7}Ga_{21.0}Sn_{8.8}Se_{51.5}$
Z	4
Structure type	α-TlSe
Crystal system	Tetragonal
Space group, Pearson symbol	*I*4/*mcm* (no. 140), *tI*16
Unit cell parameters	
a, Å	8.095(1)
c, Å	6.402(1)
Unit cell volume *V*, Å^3	419.5(2)
Number of formula units per cell *Z*	4
Calculated density, g cm^{-3}	5.99
Absorption coefficient μ, mm^{-1}	48.6
Radiation/wavelength, Å	Mo$K\alpha$/0.71073
Diffractometer	STOE IPDS II
Absorption correction	Multi-scan (PLATON [24])
θ range, °	3.6–29.0
hkl indices range	$-10 \le h \le 10$, $-10 \le k \le 11$, $-8 \le l \le 7$
Collected reflections	1793
Independent reflections/R_{int}/R_σ	167/0.060/0.131
Reflections with $I > 2\sigma(I)$	122
Refinement	F^2
Refined parameters	10
Final $R1/wR2$ [$I > 2\sigma(I)$][a,b]	0.028/0.064
Final $R1/wR2$ (all data)[a,b]	0.043/0.066
Goodness-of-fit[c] on F^2	1.153
Largest diff. peak/hole, *e* Å^{-3}	0.93/−1.46

[a]$R1 = \Sigma||F_o| - |F_c||/\Sigma|F_o|$; [b]$wR2 = [\Sigma w(F_o^2 - F_c^2)^2/\Sigma w(F_o^2)^2]^{1/2}$, $w = [\sigma^2(F_o^2) + (0.0170P)^2 + 1.1085P]^{-1}$, where $P = (\mathrm{Max}(F_o^2, 0) + 2F_c^2)/3$; [c]$\mathrm{GoF} = S = [\Sigma w(F_o^2 - F_c^2)^2/(n_{obs} - n_{param})]^{1/2}$.

Table 2: Atomic coordinates and equivalent displacement parameters (in Å^2) for $Tl_2Ga_2SnSe_6$.[a]

Atom	Wyckoff position	*G* (site occupancy)	*x*	*y*	*z*	U_{eq}
Se	8*h*	1	0.16418(11)	1/2+*x*	0	0.0334(4)
M	4*b*	1	0	½	1/4	0.0309(4)
Tl	4*a*	0.655(5)	0	0	1/4	0.0724(7)

[a]$M = 0.655(5)\mathrm{Ga} + 0.345(5)\mathrm{Sn}$.

Table 3: Anisotropic atomic displacement parameters (in Å^2) for $Tl_2Ga_2SnSe_6$.[a,b]

Atom	$U_{11} = U_{22}$	U_{33}	U_{12}
Se	0.0329(4)	0.0344(7)	−0.0043(6)
M	0.0329(5)	0.0270(9)	0
Tl	0.0440(6)	0.1291(17)	0

[a]$M = 0.655(5)\mathrm{Ga} + 0.345(5)\mathrm{Sn}$. [b]$U^{13} = U^{23} = 0$.

Table 4: Interatomic distances (δ) and coordination numbers (CN) of atoms in the crystal structure of $Tl_2Ga_2SnSe_6$.[a]

Atoms	δ (Å)	CN	Atoms	δ (Å)	CN	Atoms	δ (Å)	CN
Tl–2 Tl	3.2010(7)	10	*M*–4 Se	2.469(1)	4	Se–2 *M*	2.469(1)	6
8 Se	3.423(1)					4 Tl	3.423(1)	

[a]$M = 0.655(5)\mathrm{Ga} + 0.345(5)\mathrm{Sn}$.

Phase analysis showed that the XRD pattern of $Tl_2Ga_2GeSe_6$ was similar to that of the tetragonal II-$TlGaSe_2$ phase (high temperature-high pressure modification) [6] with slightly different unit cell parameters. In the first stage of the treatment of the crystal structure was refined as $TlGaSe_2$ using the initial atomic coordinates of HT-$TlGaSe_2$ [6]. After accounting for the predominant orientation factor (texture) along the 0 0 1 direction, refinement of isotropic displacement parameters for Tl, Ga and Se atoms showed significantly increased values of the latter, especially for the Tl and Ga sites. Taking into account the EDX results for the elemental composition, a statistical mixture $M = 0.65$ Ga + 0.35 Ge was restrained. The R_B and B_{iso} values for the *M* and Se positions were reduced, but for Tl B_{iso} they increased. Refinement of the 4*a* site occupancy (*G*) by thallium atoms resulted in $G = 0.66$. Finally both the 4*a* and 4*b* occupancies and, afterwards, the isotropic displacement parameters for all Tl, *M*, and Se atoms were refined. Experimental, calculated and difference powder XRD profiles of the $Tl_2Ga_2GeSe_6$ sample are shown in Fig. 1. Details of the refinement are listed in Table 5, atomic coordinates and their displacement parameters in Table 6. High correlation of the refined composition with the elemental analysis was observed, despite comparatively higher B_{iso} values for Tl, caused by structural features of this structure type, since

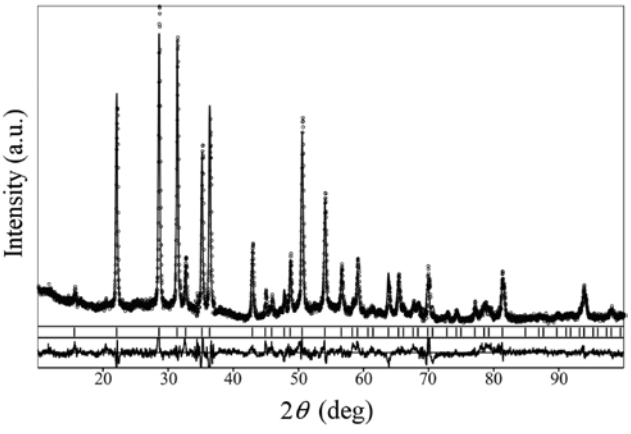

Fig. 1: Observed (dots) and calculated (line) profiles and their difference plot (bottom) of the XRD patterns of the $Tl_2Ga_2GeSe_6$ sample. Peak positions are marked by short vertical bars.

Table 5: Details of data collection and refinement of the crystal structure of $Tl_2Ga_2GeSe_6$.

Refined composition	$Tl_{1-x}Ga_{1-y}Ge_ySe_2$, $x = 0.343(5)$, $y = 0.35(2)$
Space group	*I*4/*mcm* (no. 140)
Structure type	α-TlSe
Pearson symbol and *Z*	*tI*16, 4
Unit cell parameters	
a, Å	8.0770(4)
c, Å	6.2572(5)
V, Å^3	408.20(7)
Calculated density, g · cm^{-3}	5.91
Diffractometer	DRON 4-13
Radiation/λ, Å	Cu$K\alpha$/1.54185
Mode of refinement	Full with fixed elements per cycle
2θ range/step, °	10.0–100.0/0.02
$(\sin\theta/\lambda)_{max}$, Å^{-1}	0.497
Detector	NaI(Tl) scintillation counter
Scanning time (in s) per step of 0.02° in 2θ	20
No. of reflections	69
No. of parameters (all/free)	24/5
Scale factor	0.0682(1)
Goodness-of-fit	2.46
$R_{B(I)}/R_P/R_{Pw}$, %	8.4/4.1/5.8

Table 6: Refined atomic coordinates and isotropic displacement parameters for $Tl_2Ga_2GeSe_6$.[a]

Atom	Wyckoff position	*G* (site occupancy)	*x*	*y*	*z*	B_{iso} (Å^2)
Se	8*h*	1	0.1577(2)	*x*+½	0	1.18(7)
M	4*b*	1	0	½	¼	2.87(12)
Tl	4*a*	0.657(5)	0	0	¼	3.48(9)

[a]*M* = 0.65(2) Ga + 0.35(2) Ge.

Tl atoms are localized in Se tunnels along the 0 0 1 direction (see Fig. 3a). Unfortunately, anisotropic displacement parameters could not be refined reliably from powder XRD due to a poor data to parameter ratio.

CCDC 1960737 ($Tl_2Ga_2SnSe_6$) and 1960739 ($Tl_2Ga_2GeSe_6$) contain the supplementary crystallographic data for this paper. These data can be obtained free of charge from The Cambridge Crystallographic Data Centre via www.ccdc.cam.ac.uk/data_request/cif.

2.5 Electronic structure calculations

Tight binding electronic structure calculations for a few idealized models of $Tl_{1-x}Ga_{1-y}Sn_ySe_2$ assuming fully occupied sites were performed with the linear-muffin-tin-orbital (LMTO) method in the atomic sphere approximation (ASA) using the Stuttgart TB-LMTO-ASA code [29]. The radii of the Wigner-Seitz spheres were assigned automatically (1.84, 1.47 and 1.39 Å for Tl, Ga, and Se, respectively) to achieve the best possible approximations to the full potentials [30]. Two additional empty spheres were necessary with a 16% overlap restriction. Basis sets of Tl 6*s*,6*p*,(5*d*), Ga 4*s*,4*p*,(3*d*), Sn 5*s*,5*p*,(4*d*) and Se 4*s*,4*p*,(3*d*) (downfolded [31] orbitals in parentheses) were employed. Scalar relativistic corrections were included in the calculations. The band structure was sampled for 1063 *k*-points in the corresponding irreducible wedge of the Brillouin zone.

2.6 UV/Vis diffuse reflectance spectroscopy

UV/Vis diffuse reflectance spectra were recorded on powder samples using an Agilent Technologies Cary 5000 UV-Vis-NIR spectrophotometer equipped with a diffuse-reflectance accessory (Praying Mantis, Harrick). A Spectralon disk was used as the reference material.

3 Results and discussion

The crystal structure of $Tl_2Ga_2SnSe_6$ is closely related to the structures of the stoichiometric 2-2-1-6 compounds and contains three main building units – MSe_4 tetrahedra, SeM_2Tl_4 trigonal prisms and $Tl@Tl_2Se_8$ bi-capped tetragonal antiprisms (Fig. 2). Atomic coordination numbers and selected interatomic distances are summarized in Table 4. The simplest structural representation appears in the form of chains of edge-sharing $[MSe_4]$ tetrahedra along [001], connected in the *ab* plane with Tl^+ cations occupying the channels (Fig. 3a). This structural arrangement is related to the one in the tetragonal quaternary selenide $Ag_2Ga_2SiSe_6$ (Fig. 4f), that exhibits a three-dimensional framework composed of corner-sharing $[(Ga/Si)Se_4]$ and $[AgSe_4]$ tetrahedra with empty cavities [17]. In the disordered crystal structure of $Ag_2Ga_2SiSe_6$ the Ga and Si atoms form a statistical mixture, while the Ag atoms partially occupy the 4*b* site. The crystal structure of the monoclinic quaternary selenide $Na_2In_2GeSe_6$ (Fig. 3d), exhibits a three-dimensional framework composed of corner-sharing $[InSe_4]$ and $[GeSe_4]$ tetrahedra with Na^+ cations occupying the voids [11]. The basic building unit of the $Na_2In_2GeSe_6$ framework is a $[In_4Ge_2Se_{16}]$ block comprised of two smaller $[In_2GeSe_9]$ units. The latter in turn consists of two $[InSe_4]$

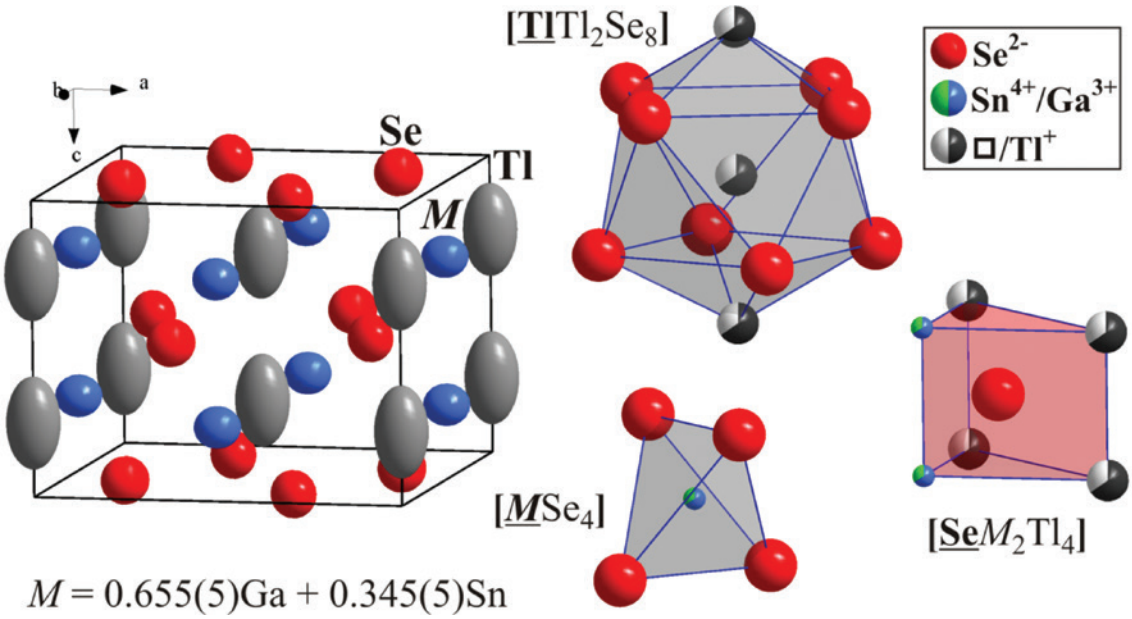

Fig. 2: Filled unit cell (atoms are shown as their anisotropic ellipsoids with 95% probability) and atomic coordination polyhedra (ions are shown as circles with color distinguishing sectors, indicating partial or mixed site occupancy) of $Tl_2Ga_2SnSe_6$.

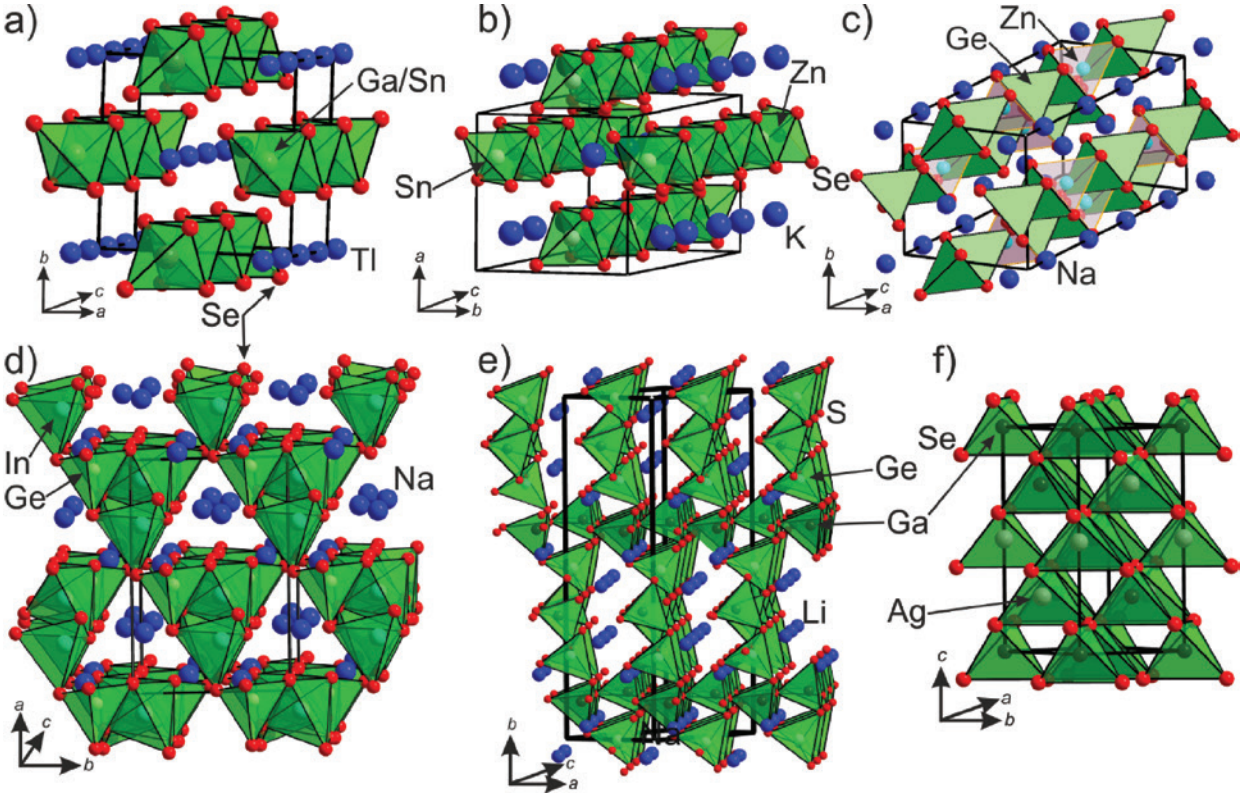

Fig. 3: Packing of tetrahedra of selenium and sulfur atoms in the crystal structures of $Tl_2Ga_2SnSe_6$ (a), $K_2Sn_2ZnSe_6$ (b) and $Na_2Ge_2ZnSe_6$ (c), $Na_2In_2GeSe_6$ (d), $Li_2Ga_2GeS_6$ (e), and $Ag_2Ga_2SiSe_6$ (f).

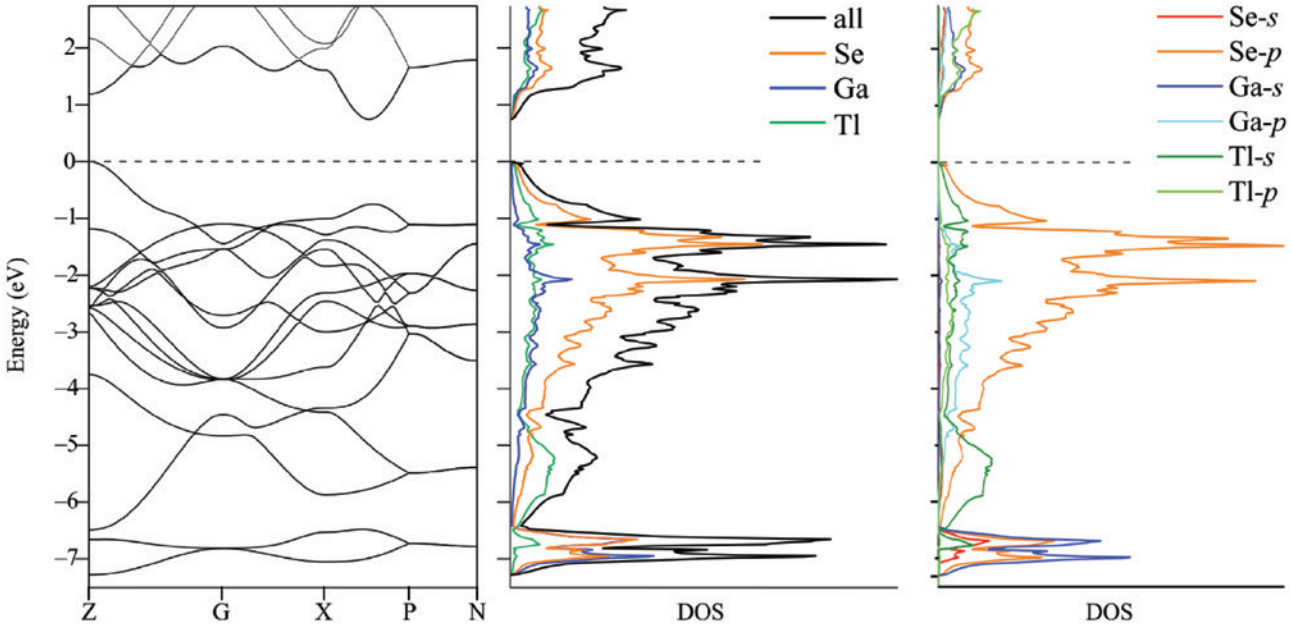

Fig. 4: Band structure and projected densities of state (DOS) for an idealized model of $Tl_2In_2SnSe_6$.

tetrahedra and one [$GeSe_4$] tetrahedron linked to each other via Se vertex-sharing. The [$In_4Ge_2Se_{16}$] blocks are connected to each other *via* corner-sharing to generate the three-dimensional framework.

The lithium sulfide $Li_2Ga_2GeS_6$ crystallizes in the non-centrosymmetric orthorhombic space group *Fdd*2 [7]. The crystal structure is built of [GeS_4] tetrahedra linked by corners to other four identical units to create a three dimensional framework with tunnels along the *c* axis, in which the Li^+ ions are located (Fig. 3e). The Li atoms in distorted tetrahedral coordination (Li@S_4) form an infinite chain parallel to the *c* axis by vertex-sharing. $K_2Sn_2ZnSe_6$ and $Na_2Ge_2ZnSe_6$ ([11], Fig. 3b and c) crystallize in the space groups *P*4/*ncc* and *I*4/*mcm*, respectively. In these structures [$SnSe_4$] or [$GeSe_4$] and [$ZnSe_4$] edge-sharing tetrahedra appear in similar chains. Two [Sn(Ge)Se_4] tetrahedra are first connected to each other by sharing two Se atoms to form the [$Sn(Ge)_2Se_6$] block, which is further linked via edge-sharing two other Se atoms with one [$ZnSe_4$] tetrahedron to build up a [$Sn(Ge)_2ZnSe_6$] infinite chain along [001]. The chains are separated from each other by K^+ or Na^+ cations occupying the voids. All K^+ and Na^+ cations are coordinated by eight Se atoms in tetragonal antiprismatic arrangement. The unit cell expansion is in good agreement with the atomic sizes of Na/Ge vs. K/Sn [32].

Observed interatomic distances indicate that in $Tl_2Ga_2SnSe_6$ thallium is monovalent (ionic radius [33] $r(Tl^+) = 1.49$ Å), gallium trivalent ($r(Ga^{3+}) = 0.62$ Å) and selenium divalent ($r(Se^{2-}) = 1.91$ Å) showing a reasonable correlation of their coordination polyhedra (Fig. 2) and earlier evaluations for β-$TlGaSe_2$ [6]. The shortest interatomic distances are those between the *M* and Se atoms indicating stronger chemical bonding between them. From the viewpoint of the charge balance each Sn atom introduced to the structure leads to simultaneous exclusion of both a Ga and a Tl atom according to $Tl^+_{1-x}Ga^{3+}_{1-y}Sn^{4+}_ySe^{2-}_2$ ($x = y = 0.345(5)$), in agreement with the observed interatomic distances (Table 4). Substitution of gallium atoms by larger tin atoms leads to an only minor expansion of the unit cell compared to the $TlGaSe_2$ analogue [6] due to partial compensation by Tl deficiency. This is further confirmed by the more visible unit cell contraction of the Ge compound (Table 5).

Electronic structure calculations were performed for a couple of slightly modified models of $Tl_2Ga_2SnSe_6$ because of the difficulties in the treatment of partially occupied sites. $TlGaSe_2$, $TlInSe_2$ and $TlSnSe_2$ have been examined in order to estimate changes in the electronic structure with regard to the atomic size, electronegativity and valence electron concentration. All three models revealed qualitatively identical results with reasonable variation of the monitored output parameters as a good approximation for the observed disordered structure. Expectedly, the fully occupied Sn position led to the shift of the Fermi level into the areas with non-zero densities of states. The proper adjustment to the corresponding valence electron count revealed a comparable gap in the electronic structure (Fig. 4). The electronic densities of state (DOS) exhibit

broad valence *s*, *p* bands reaching 8 eV below the Fermi level including large contributions from mostly Se-4*p* bands located 1–2.5 eV below E_F. In this region they exhibit the largest overlap with the Ga-4*p* and Tl-6*s*,6*p* bands. The contributions from the Ga and Tl bands are significantly smaller being comparable to each other in the range from –5 to 2 eV. This agrees well with the formally cationic roles of both metals in this compound. The Tl-6*s* bands dominate at –5 to –6.5 eV while the Ga-4s bands appear around –7 eV.

The maximum of the valence band is located at the Z point, while the pronounced minimum of the conduction band is found between the X and P points. Consequently, the model suggests an indirect band gap semiconductor with a calculated band gap size varied between the Ga and Sn model from 0.74 to 0.93 eV. These values are considerably lower than the expected range based on the samples' color and optical appearance. Since the size of the band gap is usually underestimated by the DFT methods, UV/Vis diffuse reflectance measurements were performed to obtain more accurate values. The UV/Vis diffuse reflectance spectra, recorded at room temperature, show an intense broad band with an absorption edge at 728 nm for **1** and at 779 nm for **2** (Fig. 5). These spectral features correlate well with the red-brown color of the compounds. The UV/Vis data were then employed to determine the band gap of the compounds. The values of the energy band gap (E_g) were estimated by linear extrapolation of the Tauc plot [34] [$(\alpha h\nu)^2$ vs. $h\nu$] to $(\alpha h\nu)^2 = 0$. The values of E_g are 2.15(3) eV for **1** and 2.05(5) eV for **2**, which is consistent with the transparency of the crystals and the color of the compounds. However, the band gap of **2** is smaller compared with that of **1**. A similar observation can be made in the case of other quaternary selenides, like $BaGa_2GeSe_6$ (2.22 eV) [35] and $BaGa_2SnSe_6$ (1.95 eV) [36]. It can be concluded that the heavier the employed group 14 elements is, the narrower is the band gap observed in this series of compounds. This can be explained in terms of differences

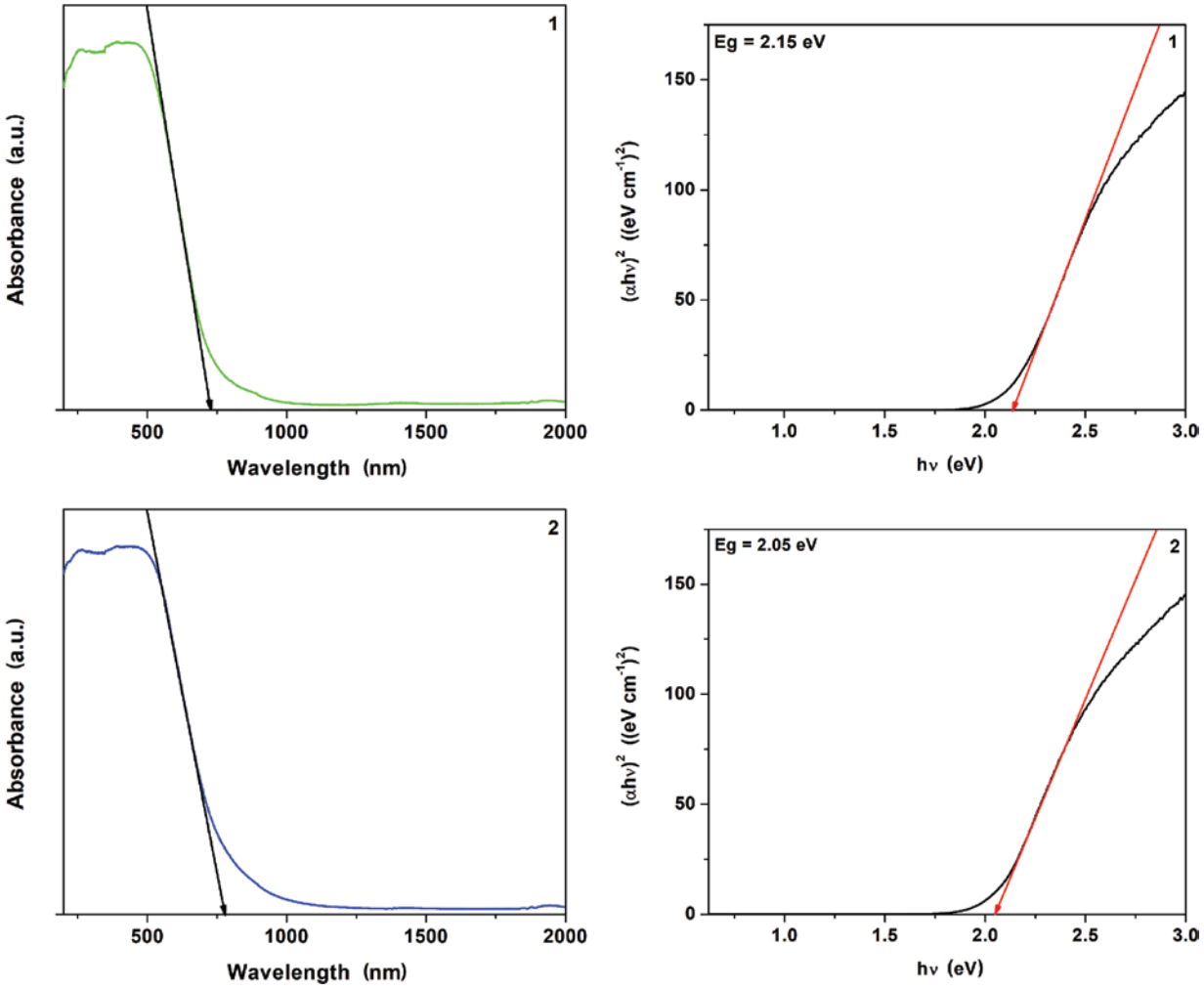

Fig. 5: UV/Vis diffuse reflectance spectra and energy band gap of **1**–**2**.

in electron binding capacities of the various ions. Nuclei of heavier tetravalent ions are larger and exhibit weaker electron binding capacities than those of lighter ones. Therefore, the valence orbitals of the heavier tetravalent ions contribute to the bottom of the conduction bands to a larger extent, resulting in smaller band gaps.

4 Conclusions

In summary, two new quaternary selenides $Tl^{+}_{1-x}Ga^{3+}_{1-y}Tt^{4+}_{y}Se^{2-}_{2}$ (Tt = Ge, Sn; $x = y = 0.345(5)$) have been synthesized from self-flux allowing growth of large single phase samples. They crystallize tetragonally in the space group $I4/mcm$ and represent a pseudoternary positionally ordered variant of the α-TlSe structure type. Intercalation of a tetrel element into the crystal structure leads to a partial substitution of the triel position and simultaneously to an equimolar exclusion of thallium. First-principle calculations and optical measurements indicate these materials to be narrow gap semiconductors suggesting further examination of their heat transport and thermoelectric performance.

Acknowledgments: The authors thank W. Hölle (MPI FKF, Stuttgart) for X-ray intensity data collection. AVM and VS would like to thank Energimydigheten, the Swedish Energy Agency for support.

References

[1] R. S. Itoga, C. R. Kannewurf, *J. Phys. Chem. Solids* **1971**, *32*, 1099.
[2] A. M. Ulubey, F. M. Hashimzade, D. A. Huseinova, M. A. Nizametdinova, G. S. Orudzhev, K. R. Allakhverdiev, N. T. Yıldız, *Phys. Status Solidi B* **2011**, *248*, 181.
[3] C. R. Whitehouse, A. A. Balchin, *J. Mater. Sci.* **1978**, *13*, 2394.
[4] T. Isaacs, *Z. Kristallogr.* **1975**, *141*, 104.
[5] D. Müller, F. E. Poltmann, H. Hahn, *Z. Naturforsch.* **1974**, *29b*, 117.
[6] K.-J. Range, G. Mahlberg, S. Obenland, *Z. Naturforsch.* **1977**, *32b*, 1354.
[7] Y. Kim, I. Seo, S. W. Martin, J. Baek, P. S. Halasyamani, N. Arumugam, H. Steinfink, *Chem. Mater.* **2008**, *20*, 6048.
[8] W. Yin, K. Feng, W. Hao, J. Yao, Y. Wu, *Inorg. Chem.* **2012**, *51*, 5839.
[9] S.-F. Li, B.-W. Liu, M.-J. Zhang, Y.-H. Fan, H.-Y. Zeng, G.-C. Guo, *Inorg. Chem.* **2016**, *55*, 1480.
[10] G. E. Delgado, A. J. Mora, F. V. Pérez, J. González, *Cryst. Res. Technol.* **2007**, *42*, 663.
[11] M. Zhou, C. Li, X. Li, J. Yao, Y. Wu, *Dalton Trans.* **2016**, *45*, 7627.
[12] G. Li, Q. Liu, K. Wu, Z. Yang, S.-L. Pan, *Dalton Trans.* **2017**, *46*, 2778.
[13] J. P. Yohannan, K. Vidyasagar, *J. Solid State Chem.* **2016**, *238*, 147.
[14] V. P. Sachanyuk, G. P. Gorgut, V. V. Atuchin, I. D. Olekseyuk, O. V. Parasyuk, *J. Alloys Compd.* **2008**, *452*, 348.
[15] I. D. Olekseyuk, V. P. Sachanyuk, O. V. Parasyuk, *J. Alloys Compd.* **2006**, *414*, 73.
[16] O. V. Krykhovets, L. V. Sysa, I. D. Olekseyuk, T. Glowyak, *J. Alloys Compd.* **1999**, *287*, 181.
[17] M. Piasecki, G. L. Myronchuk, O. V. Parasyuk, O. Y. Khyzhun, A. O. Fedorchuk, V. V. Pavlyuk, V. R. Kozer, V. P. Sachanyuk, A. M. El-Naggar, A. A. Albassam, J. Jedryka, I. V. Kityk, *J. Solid State Chem.* **2017**, *246*, 363.
[18] O. V. Parasyuk, V. V. Pavlyuk, O. Y. Khyzhun, V. R. Kozer, G. L. Myronchuk, V. P. Sachanyuk, G. S. Dmytriv, A. Krymus, I. V. Kityk, A. M. El-Naggar, A. A. Albassam, M. Piasecki, *RSC Adv.* **2016**, *6*, 90958.
[19] V. P. Sachanyuk, I. D. Olekseyuk, O. V. Parasyuk, *J. Alloys Compd.* **2007**, *443*, 61.
[20] G. E. Davydyuk, O. Y. Khyzhun, A. H. Reshak, H. Kamarudin, G. L. Myronchuk, S. P. Danylchuk, A. O. Fedorchuk, L. V. Piskach, M. Y. Mozolyuk, O. V. Parasyuk, *Phys. Chem. Chem. Phys.* **2013**, *15*, 6965.
[21] B. Eisenmann, A. Hofmann, *Z. Kristallogr.* **1991**, *195*, 318.
[22] P. Capper, P. Rudolph (Eds.), *Crystal Growth Technology. Semiconductors and Dielectrics*, Wiley-VCH, Weinheim, **2011**.
[23] L. J. Farrugia, *J. Appl. Crystallogr.* **1999**, *32*, 837.
[24] A. L. Spek, *J. Appl. Crystallogr.* **2003**, *36*, 7.
[25] M. C. Burla, R. Caliandro, B. Carrozzini, G. L. Cascarano, C. Cuocci, C. Giacovazzo, M. Mallamo, A. Mazzone, G. Polidori, *J. Appl. Crystallogr.* **2015**, *48*, 306.
[26] G. M. Sheldrick, *Acta Crystallogr.* **2015**, *C71*, 3.
[27] K. Brandenburg, DIAMOND (version 2.1c), Crystal and Molecular Structure Visualization, Crystal Impact – H. Putz & K. Brandenburg GbR, Bonn (Germany) **1999.**
[28] L. Akselrud, Y. Grin, WINCSD (version 4), Software Package for Crystallographic Calculations, Max-Planck-Institut für Chemische Physik fester Stoffe, Dresden (Germany) **2014**. See also: L. Akselrud, Y. Grin, *J. Appl. Crystallogr.* **2014**, *47*, 803.
[29] O. Jepsen, O. K. Andersen, The Stuttgart TB-LMTO-ASA programm (version 4.7), Max-Plank-Institut für Festkörperforschung, Stuttgart (Germany) **2000**.
[30] O. Jepsen, O. K. Andersen, *Z. Phys. B* **1995**, *97*, 35.
[31] W. R. Lambrecht, O. K. Andersen, *Phys. Rev. B* **1986**, *34*, 2439.
[32] B. Cordero, V. Gomez, A. E. Platero-Prats, M. Reves, J. Echeverria, E. Cremades, F. Barragan, S. Alvarez, *Dalton Trans.* **2008**, *21*, 2832.
[33] J. Emsley, *The Elements*, 3rd ed., Clarendon Press, Oxford, **1998**.
[34] J. Tauc, R. Grigorovici, A. Vancu, *Phys. Status Solidi B* **1966**, *15*, 627.
[35] W. Yin, K. Feng, R. He, D. Mei, Z. Lin, J. Yao, Y. Wu, *Dalton Trans.* **2012**, *41*, 5653.
[36] X. Li, C. Li, P. Gong, Z. Lin, J. Yao, Y. Wu, *J. Mater. Chem. C* **2015**, *3*, 10998.